Production of evaporation residues in the vicinity of the N=126 closure

Roman Sagaidak

Flerov Laboratory of Nuclear Reactions, Joint Institute for Nuclear Research, 141980, Dubna, Moscow region, Russian Federation

E-mail: sagaidak@nrmail.jinr.ru

Abstract. The shell structure and fission-barrier heights of nuclei involved in the compound-nucleus (CN) de-excitation chains leading to observable evaporation residues (ER) determine essentially fusion-evaporation cross sections for heavy fissile nuclei produced in the vicinity of the N=126 neutron shell in heavy ion (HI) reactions. The entrance-channel effect of quasi-fission (QF) lowering the fusion cross section in reactions with massive nuclei and the effect of the collective enhancement in the nuclear level density (CENLD), corresponding to the exit channel, should strongly reduce production cross sections for ER and increase the observed fission cross section in the vicinity of N=126. These effects were not evidently manifested in the analysis of cross sections obtained in different CN reactions leading to Po isotopes produced in a wide region of N. This analysis has been performed in the framework of standard statistical model (SSM) approximations. As a whole, production cross sections for neutron deficient Po nuclei produced in HI reactions can be reproduced in the framework of SSM with the reduced liquid-drop fission barriers [1]. We present a similar analysis of ER and fission cross section data obtained in the reactions induced by ^{3,4}He on Pb and Bi targets, which lead to Po and At compound nuclei [2], which proved to be a good test of the preceding results [1]. Such reactions are characterized by much lower angular momenta transferred to a CN that allows to suggest more pronounced manifestation of CENLD effects in the CN decay. These reactions also do not reveal any indications of QF. This simplifies the data analysis and makes it more unambiguous. The results of the analysis of the ^{3,4}He reactions performed in the present work demonstrate the same changes in the fission barrier heights for Po and At nuclei as obtained earlier with HI reactions data [1].

1. Introduction

A comparison of fission barrier heights calculated in a region between two neutron shell numbers ($126 \lesssim N \lesssim 184$) reveals a large spread in their predictions for exotic neutron-rich nuclei [3]. At the same time, reasonable description of the fission barrier heights close to the stability line (where the model parameters were tuned to the experimental data) is accomplished [4]. Large deviations between predictions of different models and the fission barrier heights derived from nuclear reaction data were pointed out earlier for neutron-deficient nuclei [5]. The difference between calculations for extremely neutron-rich (hypothetical) nuclei reaches more than 30 MeV. Such uncertainty results in completely different scenarios as far as the r-process termination by fission is considered [6]. In macroscopic calculations of fission barriers, the height of the barrier is proportional to the nuclear surface energy which, in turn, depends on the charge asymmetry parameter $I = (N - Z)/A$. Therefore, the study of the isotopic dependence of fission-barrier

heights for nuclei far from the stability line is one of the most important tasks in modern fission studies. Unfortunately, these studies for neutron-rich nuclei are very difficult due to their very low production rates as it follows, e. g., from the results obtained in relativistic HI collisions [7] and as one may expect from calculations exploring nuclear transfer reactions at Coulomb energies [8]. At the same time, the isotopic dependence of fission barrier heights can be presently studied in the more readily accessible region of neutron-deficient nuclei produced in HI fusion-evaporation reactions.

2. Statistical model considerations of ER production in HI fusion reactions

Production cross sections for the neutron-deficient Po to Th nuclei, obtained in very asymmetric projectile-target fusion-evaporation reactions are mainly determined by level density parameters and the fission-barrier heights for nuclei involved in the CN de-excitation chains. Analysis of the measured ER cross sections is usually performed in the framework of the SSM approximations, e.g., with HIVAP [9] using the liquid-drop (LD) fission barrier heights with scaling of the form: $B_{\rm f}(L) = k_{\rm f}B_{\rm f}^{\rm LD}(L) - \Delta W_{\rm gs}$ ($k_{\rm f}$ is a scaling factor at the rotating LD barriers $B_{\rm f}^{\rm LD}(L)$ [10] and $\Delta W_{\rm gs}$ is the ground state shell correction). The macroscopic components of the barriers $B_{\rm f}^{\rm m} = k_{\rm f}B_{\rm f}^{\rm LD}$ derived from such analysis of the measured cross sections for Fr and Ra nuclei production [11]–[14] are compared to various predictions in Fig. 1. The derived values are lower than any calculations [15] (with the exception of [16]) and are a relatively smooth function of N, e.g., for Fr nuclei, $k_{\rm f}$ is gradually reduced from 0.85 to 0.8, in going from N=131 to 117. Prior analysis of ER and fission cross sections for Po nuclei in a wide region of $105 \leqslant N \leqslant 126$ [1] shows a sizable decrease in $B_{\rm f}^{\rm m}$ as compared to any predictions (see Fig. 1). This analysis includes ER cross section data obtained in nearly symmetric and asymmetric reactions leading to the most neutron-deficient Po nuclei. The possibility of QF effects leading to the fusion probability $P_{\rm fus} < 1$ cannot be ruled out in these reactions bearing in mind, e.g., the comparison of the ER production cross sections obtained in the ^{16}O+^{186}W and ^{48}Ca+^{154}Sm reactions leading to the ^{202}Pb* CN [18]. Such comparison indicates the $P_{\rm fus} < 1$ values [19], which are noticeably differed from similar values obtained with measured fission cross section and in calculations.

Note that the macro-microscopic models [3, 15] imply a smooth behavior of $B_{\rm f}^{\rm m}$ observed for Fr and Ra (Fig. 1). It has to be also mentioned that any manifestations of the CENLD effects do not imply the data derived in Fig. 1. In particular, these effects are expected to be strongly pronounced in the vicinity of the N=126 spherical shell as the drop of ER production cross sections as it follows, e.g., from the model presented in [7]. Such effect is not observed in the cross section data of fusion experiments and, respectively, it is not revealed with the SSM analysis as an expected relative reduction in the $B_{\rm f}^{\rm m}$ values (HIVAP does not take into account the CENLD effects).

Among other peculiarities in the ER production cross sections, the effect of the energy losses of a massive HI inside the target of finite thickness deserves attention. The effect leads to visible broadening of excitation functions along with lowering of their maxima. It has to be taken into account when the calculated excitation functions are adjusted to the measured one using variations in the macroscopic fission barrier heights [20]. Lastly, the reliability of the ER production cross sections measured in very asymmetric combinations implying a negligible fusion suppression may be of great importance for the derived $B_{\rm f}^{\rm m}$ values. For example, available ER cross section data obtained in the ^{197}Au(^{12}C,xn)$^{209-x}$At reactions (see Refs in the most recent works [21]) demonstrate a difference in the values corresponding to a factor of 5–6 that leads to the difference in the "adjusted" $k_{\rm f}$ values in the range between 0.5 and 1.0 as it follows from the analysis with HIVAP.

3. Analysis of cross section data obtained in ^{3,4}He+Pb,Bi reactions

The He induced reactions on Pb and Bi targets, which lead to Po and At compound nuclei, can be particularly suited for this study considering the above mentioned difficulties inherent in the analysis of HI reaction cross sections. These reactions have at least two advantages over HI ones: a) much lower angular momenta are transferred to compound nuclei formed in the reactions ensuring, along with relatively high excitation energies, more favorable conditions for the manifestation of the CENLD effects as compared to the HI ones [1] associated with very high rotation energies and b) these reactions reveal no indications of QF due to the ultimate difference in the masses of projectiles and targets.

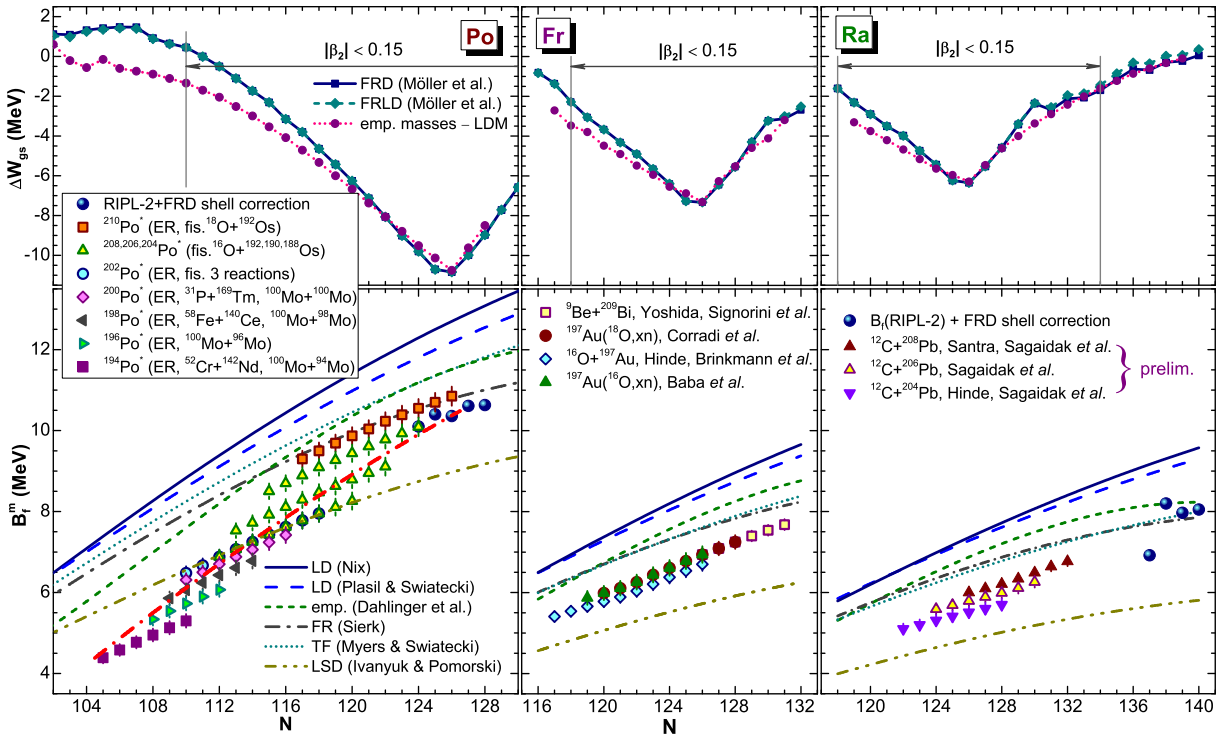

Figure 1. Bottom panels: the macroscopic fission barriers $B_{\rm f}^{\rm m}$ for Po [1], Fr and Ra nuclei derived with the SSM [9] analysis of ER and fission excitation functions obtained in HI fusion reactions (symbols) in comparison to the different model predictions [5, 15, 16] (lines). Upper panels: the ground-state shell corrections $\Delta W_{\rm gs}$ with the indicated regions of nearly spherical nuclei around N=126, corresponding to $|\beta_2| < 0.15$ [17].

Earlier, the fission barrier heights of Po and At nuclei (along with other parameters which determined the CN statistical decay) were derived using the only fission reactions induced by light charged particles (including He) on corresponding target nuclei [22]–[25]. At present, available experimental data on the production cross sections of Po and At ER produced in (^{3,4}He, xn) reactions [2] allow simultaneous analysis of the evaporation and fission cross section data as was done earlier [1] for some HI data. The main difference of the present approach from the previous fission data analysis [22]–[25] is the derivation of the nuclear potential parameters which are sensitive to the ER cross section data at barrier and sub-barrier energies, whereas fission data are more sensitive to the CN statistical decay parameters. Earlier, the fission data analysis [23]–[25] was performed using fusion cross sections *calculated* with the optical model.

The most representative experimental data were obtained in the ^{4}He+^{208}Pb reaction as shown in Fig. 2 for the 1n to 4n evaporation channels. The 1n and 2n evaporations allow choosing definitely the main parameter values of the nuclear exponential potential (V_0, r_0 and $\sigma(r_0)/r_0$)

which is used in the previous analysis of the HI Po data [1]. The evaporation data indicate importance of γ-emission at the CN de-excitation. Fission data (Fig. 3) are more sensitive to the level-density and fission barrier scaling parameters (a_ν, a_f/a_ν and k_f) of SSM. At high energies the critical angular momentum for fusion L_cr becomes a crucial value determining cross sections calculated for fission and for the $6n$ to $10n$ evaporations.

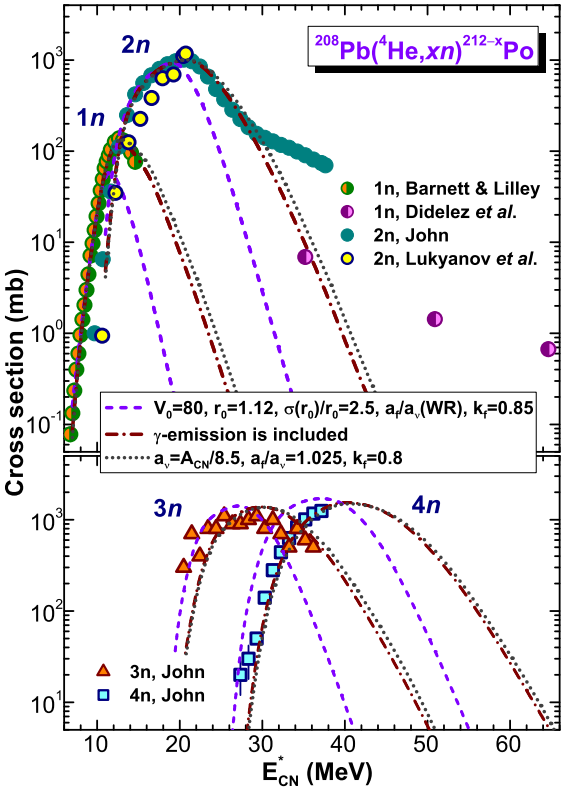

Figure 2. The $^{211-208}$Po isotopes production cross sections measured in the ^{208}Pb(^{4}He, $1n$–$4n$) reactions by different groups are shown by symbols (see Refs. in [2]). The corresponding excitation functions obtained with the SSM calculations using the best choice of the nuclear potential parameters and different sets of the CN-decay parameters are shown by lines.

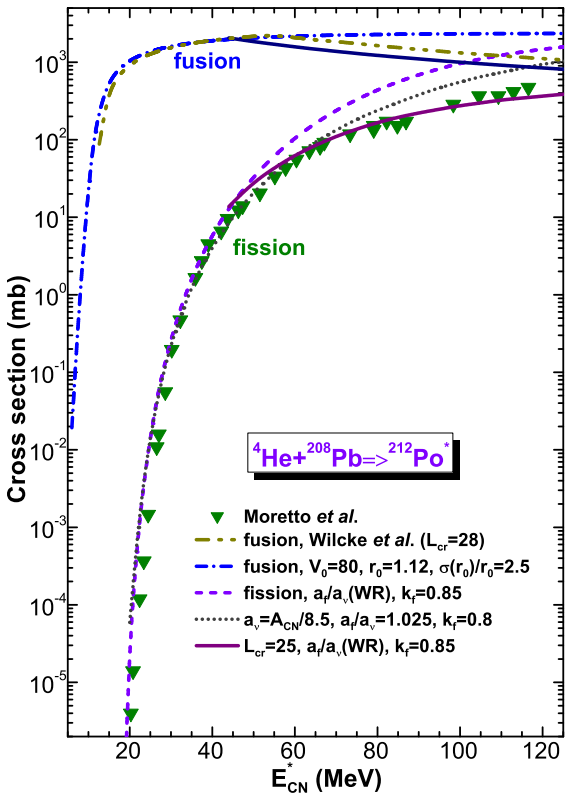

Figure 3. Fission cross sections measured in the ^{4}He+^{208}Pb reaction [24] (triangles) are shown together with the fission excitation functions calculated in the same as in Fig. 2 and with use of $L_\mathrm{cr} = 25$ (lines). Fusion cross sections tabulated in [26] as well as calculated with the nuclear exponential potential are also shown for the reference.

In Table 1, the main parameters of the nuclear exponential potential and of the statistical decay of Po and At compound nuclei (see more details in [1]) are shown. Their values were varied within the SSM [9] data analysis and that corresponded to the best fit of calculations to the data [2] are indicated in Table 1. In the SSM description of the CN decay the preference was given to the values of the level density parameters calculated according to [9] and designated as a_f/a_ν(WR). The same approach was used earlier [1], although excitation functions calculated with $a_\nu = 8.5/A$ and $a_\mathrm{f}/a_\nu = 1.05$ are very close to those corresponding to a_f/a_ν(WR).

In Table 2, as examples, the values of maxima and their positions for the xn-evaporation cross sections obtained in the most representative ^{4}He+Pb,Bi data [2] and in the corresponding SSM calculations with the parameter values listed in Table 1 are compared. Note that these calculations show a good fit to the measured fission cross sections (see Fig. 3).

In Fig. 4 the Po and At macroscopic fission barriers derived with the present analysis of

Table 1. The nuclear exponential potential and CN decay main parameters which were varied within the present SSM [9] data analysis. The values correspond to the best fit to the data [2].

Projectile	Target	V_0 (MeV/fm)	r_0 (fm)	$\sigma(r_0)/r_0$ (%)	$L_{\rm cr}$ ($\hbar$)	$a_{\rm f}/a_\nu$[9]	$k_{\rm f}$	$L_{\rm cr}$ [26] ($\hbar$)
^{4}He	$^{208-206,204}$Pb	80	1.12	2.5	25	1.068–1.066	0.85	28
	^{209}Bi			3.5	26	1.0621		
^{3}He	^{208,207}Pb	60	1.25	8.5	16	1.068, 1.066		18
	^{209}Bi					1.0615		

Table 2. The values of maxima and their positions corresponding to the CN excitation energy for the (^{4}He,xn)-excitation functions obtained in experiments [2] (two upper lines) and in the present calculations using [9] with parameter values listed in Table 1 (next two bottom lines).

		Cross section maximum (mb) / Position of maximum (MeV)									
Target		$1n$	$2n$	$3n$	$4n$	$5n$	$6n$	$7n$	$8n$	$9n$	$10n$
^{208}Pb	Expt	135	1010	∼1100	>1250		830	930	∼400	242	142
		12.6	20.5	∼30	>37		60.7	75.4	∼87	102.4	111.7
	Calc	130	1040	1460	1610	1290	1020	730	550	377	256
		13	21	30	40	52	63	75	86	100	113
^{206}Pb	Expt		1050	>1380	>1270	1020	521	340	320	305	
			25	>30	>41	58.4	76.0	80.9	93.7	112.8	
	Calc	205	1020	1440	1560	1270	935	710	490		
		15	22	32	42	53	65	77	89		
^{209}Bi	Expt	144	954	1300	1090	736	603				
		12.3	21.2	27.7	40.5	55.0	63.4				
	Calc	202	1100	1400	1530	1280	980	640			
		13	22	31	42	53	65	76			

ER and fission excitation functions obtained in the ^{3,4}He fusion reactions are shown. As in the similar case of the HI reaction data analysis [1], the heights of the barrier in the region of $114\leqslant N \leqslant 128$ are lower than any calculations [15] (with the exception of calculations in the framework of the LSD-model [16]).

4. Summary

ER and fission cross sections measured for ^{3,4}He reactions leading to the Po and At compound nuclei are analyzed in the framework of the Standard Statistical Model. This latter allows to reproduce reasonable well the cross sections in both channels. The macroscopic fission barriers derived for these nuclei are found lower than the calculated ones with different models, with the exception of those predicted by the LSD model [16] which underestimates the data. The same behavior has been observed earlier with HI- reaction data. Furthermore, the fission barriers for Po nuclei are in satisfactory agreement with those extracted from other authors with a similar SSM data analysis of very asymmetric HI-fusion reactions. These findings indicate that ^{3,4}He reactions can be used to verify the results of the HI data analysis using a similar approach, and that the derived macroscopic fission barriers (along with other SSM parameters) can provide an estimate of the fusion probability in more symmetric reactions

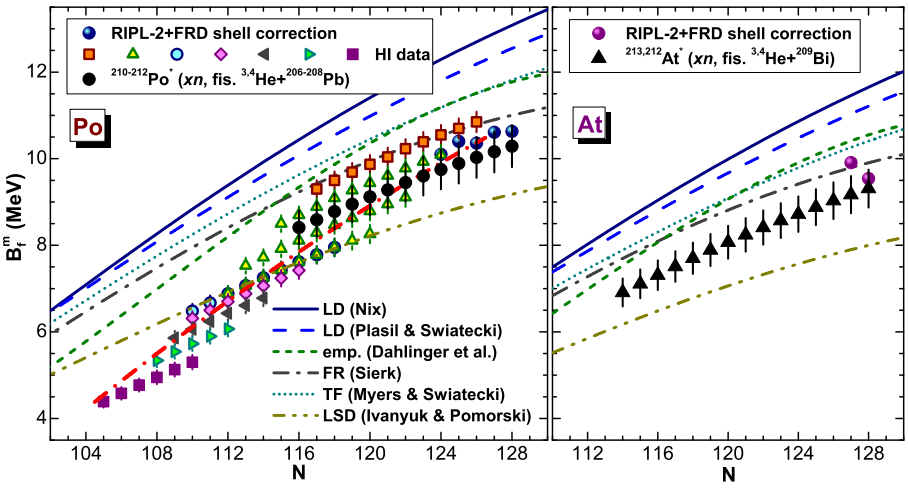

Figure 4. The same as in Fig 1 but for the Po and At macroscopic barriers derived with the analysis of ER and fission excitation functions obtained in ^{3,4}He fusion reactions (black symbols).

Acknowledgments

This work was partially supported by the RFBR Grant 13-02-12052.

References

[1] Sagaidak R N and Andreyev A N 2009 *Phys. Rev.* C **79** 054613
[2] Experimental Nuclear Reaction Data (EXFOR) `http://www.nndc.bnl.gov/exfor/exfor.htm`
[3] Mamdouh A, Pearson J M, Rayet M and Tondeur F 2001 *Nucl. Phys.* A **679** 337
[4] Belgya T *et al* 2006 *Handbook for calculations of nuclear reaction data, RIPL-2* IAEA-TECDOC-1506, `https://www-nds.iaea.org/ripl-2/`
[5] Dahlinger M, Vermeulen D and Schmidt K-H 1982 *Nucl. Phys.* A **376** 94
[6] Panov I V, Kolbea E, Pfeiffer B, Rauscher T, Kratz K-L and Thielemann F-K 2005 *Nucl. Phys.* A **747** 633
[7] Junghans A R, de Jong M, Clerc H-G, Ignatyuk A V, Kudyaev G A and Schmidt K H 1998 *Nucl. Phys.* A **629** 635
[8] Zagrebaev V I and Greiner Walter 2013 *Phys. Rev.* C **87** 034608
[9] Reisdorf W 1981 *Z. Phys.* A **300** 277; Reisdorf W and Schädel M 1992 *Z. Phys.* A **343** 47
[10] Cohen S, Plasil F and Swiatecki W J 1974 *Ann. of Phys.* **82** 557
[11] Corradi L. *et al* 2005 *Phys. Rev.* C **71** 014609
[12] Hinde D J, Berriman A C, Butt R D, Dasgupta M, Gontchar I I, Morton C R, Mukherjee A and Newton J O 2002 *J. Nucl. Rad. Sci.* **3** 31.
[13] Sagaidak R N *et al* 2003 *Phys. Rev.* C **68** 014603.
[14] Santra S, Singh P, Kailas S, Shrivastava A and Mahata K 2001 *Phys. Rev.* C **64** 024602
[15] Nix J R 1969 *Nucl. Phys.* A **130** 241; Plasil F and Swiatecki W J 1973 in Vandenbosch R and Huizenga J R *Nuclear fission* (New York: Academic Press) p 246; Sierk A J 1986 *Phys. Rev.* C **33** 2039; Myers W D and Świątecki W J 1999 *Phys. Rev.* C **60** 014606
[16] Ivanyuk F A and Pomorski K 2009 *Phys. Rev.* C **79** 054327
[17] Möller P, Nix J R, Myers W D and Swiatecki W J 1995 *At. Data Nucl. Data Tables* **59** 185
[18] Stefanini A M *et al* 2005 *Eur. Phys. J.* A **23** 473
[19] Sagaidak R N 2012 *EPJ Web of Conferences* **21** 06001
[20] Sagaidak Roman and Andreyev Andrei 2014 *Int. J. Modern Phys.* E **23** 1450001
[21] Cavinato M *et al* 1995 *Phys. Rev.* C **52** 2577; Joosten R *et al* 2000 *Phys. Rev. Lett.* **84** 5066
[22] Becchetti F D, Hicks K H, Fields C A, Peterson R J, Raymond R S, Ristinen R A, Ullmann J L and Zaidins C S 1983 *Phys. Rev.* C **28** 1217
[23] Ignatyuk A V, Smirenkin G N, Itkis M G, Mulgin S I, and Okolovivh V N 1985 *Sov. J. Part. Nucl.* **16** 307
[24] Moretto L G, Jing K X, Gatti R, Wozniak G J and Schmitt R P 1995 *Phys. Rev. Lett* **75**, 4186
[25] Rubehn Th, Jing K X, Moretto L G, Phair L, Tso K, and Wozniak G J 1996 *Phys. Rev.* C **54** 3062
[26] Wilcke W W, Birkelund J R, Wollersheim H J, Hoover A D, Huizenga J R, Schröder W U and Tubbs L E 1980 *At. Data Nucl. Data Tables* **25** 391